IRSTI 31.25.19 https://doi.org/10.26577/IJBCh202619111

E.F. Aliyeva*, N.T. Rahimli, N.A. Zeynalov

Laboratory of Nanostructured metal-polymer catalysts, Ministry of Science and Education Republic of Azerbaijan, Institute of Chemistry PLE, Baku, Azerbaijan
*e-mail: elmira.aliyeva@kqki.science.az

COMPARATIVE EFFECT OF APS AND AIBN INITIATORS ON GUM ARABIC-ACRYLAMIDE HYDROGEL SYNTHESIS AND PROPERTIES

Abstract: This study investigates the influence of radical initiator chemistry on the synthesis and structural evolution of pH-responsive gum arabic–acrylamide (GA-g-AM) hydrogels intended for drug-delivery applications. Gum arabic was used as a natural polysaccharide backbone, and acrylamide was grafted via a free-radical mechanism to form crosslinked hydrogel networks. A controlled comparative evaluation of ammonium persulfate (APS) and azobisisobutyronitrile (AIBN) was performed under identical synthesis conditions to evalute the specific influence of initiator type on hydrogel network formation. FTIR, SEM, and XRD analyses confirmed successful copolymerization and revealed differences in structural organization and packing density between the two systems. Swelling experiments demonstrated clear pH-responsive behavior, with maximum equilibrium swelling observed at pH 2. APS-initiated hydrogels exhibited an equilibrium swelling of 720 ± 5%, whereas AIBN-initiated systems reached 1026 ± 5%, indicating differences in crosslink distribution and internal network structure. APS-generated hydrogels showed a more compact morphology, while AIBN-based systems formed comparatively looser networks with higher water uptake. Overall, the results indicate that APS promotes the formation of structurally more organized and compact GA-based hydrogel networks, highlighting the decisive role of initiator chemistry in tailoring natural polymer-derived drug-delivery systems.

Keywords: gum arabic, acrylamide, APS, AIBN, graft copolymerization, hydrogel swelling.

Introduction

Polymer grafting represents a widely used molecular engineering strategy for tailoring the physicochemical and functional properties of polymeric materials, including solubility, morphology, mechanical stability, and biological compatibility (Bhattacharya & Misra, 2004; Przesławski et al., 2022; Purohit et al., 2023; Vega-Hernández et al., 2021). By introducing side chains onto pre-existing macromolecular backbones, grafting enables controlled modification of intermolecular interactions and network architecture, thereby directly influencing swelling behavior, diffusion pathways, and structural integrity (Bhattacharya & Misra, 2004; Gola et al., 2021; Przesławski et al., 2022; Purohit et al., 2023). Among different approaches, free-radical grafting remains particularly attractive due to its operational simplicity, compatibility with aqueous media, and applicability to natural polymers (Bhattacharya & Misra, 2004; Odian, 2004; Purohit et al., 2023; Vega-Hernández et al., 2021).

In free-radical grafting systems, initiators play a decisive role because they generate reactive radical species that activate either the polymer backbone or the monomer, enabling chain initiation and propagation. Thermal decomposition of persulfate or azo initiators produces radicals capable of initiating polymerization and crosslinking reactions. Consequently, grafting efficiency, chain growth behavior, and the resulting network architecture strongly depend on the chemical nature and reactivity of the initiator employed (Bhattacharya & Misra, 2004; Odian, 2004; Purohit et al., 2023). Natural polysaccharides have attracted considerable attention as sustainable backbone materials for biomedical hydrogel systems. Among them, GA, a highly branched arabinogalactan-based polysaccharide, exhibits high hydrophilicity, biodegradability, biocompatibility, and abundant hydroxyl functional groups suitable for radical activation (Ali et al., 2009;

Amaya-Chantaca et al., 2022; Etxabide et al., 2018; Verbeken et al., 2003). Structurally, GA contains multiple reactive functional moieties, including hydroxyl (–OH), carboxyl (–COOH), and glycosidic ether linkages, which provide potential sites for hydrogen abstraction and macroradical formation during graft polymerization (Etxabide et al., 2018; Verbeken et al., 2003). GA-based materials have therefore been explored in controlled drug delivery, bioactive composites, adsorption systems, and release-regulated formulations (Amaya-Chantaca et al., 2022; Etxabide et al., 2018; Hoffman, 2012; Li & Mooney, 2016; Peppas et al., 2000; Saber-Samandari et al., 2013). However, the intrinsic structural heterogeneity and limited mechanical robustness of native GA restrict its direct use as a stable drug carrier matrix, making graft modification necessary to improve structural integrity and regulate swelling behavior (Hoffman, 2012; Li & Mooney, 2016; Peppas et al., 2000).

AM is widely employed in hydrogel engineering because of its strong radical polymerization reactivity, hydrophilicity, and ability to form mechanically stable poly(acrylamide) networks (Cao et al., 2011; Çankaya, 2016; Madduma-Bandarage & Madihally, 2021; Zaharia et al., 2024). The vinyl double bond (C=C) of AM actively participates in radical polymerization, while its amide group (–$CONH_2$) promotes hydrogen bonding and water retention, both essential for drug loading capacity and controlled release performance (Cao et al., 2011; Madduma-Bandarage & Madihally, 2021).

Polymer grafting can be achieved through several mechanisms, including the grafting-to, grafting-from, and grafting-through strategies (Bhattacharya & Misra, 2004; Cummings et al., 2019; Purohit et al., 2023; Vega-Hernández et al., 2021). In the grafting-from approach, initiating sites are generated directly on the backbone and polymer chains propagate in situ, enabling higher grafting density and efficient network formation (Bhattacharya & Misra, 2004; Cummings et al., 2019). In the present work, AM was grafted onto GA via a grafting-from mechanism in the presence of the crosslinker N,N′-methylene bisacrylamide (MBAA).

Among commonly used radical initiators, APS and AIBN exhibit fundamentally different radical generation mechanisms. APS contains a persulfate peroxide bond (–O–O–) that thermally cleaves to generate highly reactive sulfate radicals capable of abstracting hydrogen atoms from hydroxyl groups on polysaccharide backbones, thereby producing active grafting sites and promoting backbone-initiated polymer growth. In contrast, AIBN contains an azo functional group (–N=N–) which decomposes thermally with nitrogen release to form carbon-centered radicals that primarily attack the vinyl double bond of acrylamide and initiate chain propagation from the monomer phase (Odian, 2004; Purohit et al., 2023). Because APS promotes both backbone activation and monomer initiation whereas AIBN mainly initiates monomer polymerization, these initiators may lead to different grafting densities, crosslink distributions, and hydrogel morphologies (Cummings et al., 2019; Işıver & Saraydın, 2021; Jabeen et al., 2022; Naushad et al., 2019; Noordergraaf et al., 2018).

Despite the widespread use of APS and AIBN in radical polymerization systems, systematic comparative investigations focusing on their specific influence on graft copolymerization onto natural polysaccharide backbones remain scarce**.** Accordingly, the present study provides a controlled comparative evaluation of APS and AIBN in the synthesis of GA-g-AM hydrogels to assess how initiator chemistry governs grafting efficiency, network formation, swelling behavior, and structural stability relevant to drug delivery applications.

Materials and methods

GA was purchased from Carlo Erba Reagents (France). AM monomer, NNMBA, and AIBN were obtained from Central Drug House Pvt. Ltd. (India). APS was supplied by Baza N1 (China).

Grafting of Acrylamide onto Gum Arabic

The synthesis of GA - g – AM hydrogels was carried out via a free-radical graft-copolymerization reaction. AM was grafted onto GA using APS or AIBN as radical initiators in separate systems, while MBAA served as the crosslinking agent (Elbedwehy & Atta, 2020; Manaila & Craciun, 2024).

Initially, a 1% (w/v) aqueous GA solution was prepared in deionized water. Subsequently, an AM solution of identical concentration (1% w/v) was added under continuous stirring. Stock solutions of AM (1.406×10^{-1} mol L^{-1}), APS (8.76×10^{-2} mol L^{-1}), AIBN (1.218×10^{-1} mol L^{-1}), and MBAA (6.49×10^{-1} mol L^{-1}) were then introduced into the reaction mixture in predetermined amounts to obtain the desired formulation. The total reaction volume was adjusted to 100 ml.

Polymerization was conducted in a glass round-bottom reactor equipped with magnetic stirring (500

rpm) and maintained at 65 ± 5^{0}C for 3 h under ambient atmospheric conditions. For the AIBN-initiated system, AIBN was finely dispersed in the aqueous reaction mixture under continuous stirring to ensure homogeneous distribution prior to thermal decomposition.

After completion of the reaction, the obtained crosslinked hydrogels were washed repeatedly with deionized water (at least three times) to remove unreacted monomers, residual initiator, and soluble fractions. The purified samples were then dried in an oven at 40^{0}C for 24 h until a constant weight before measurements were performed.

The grafting percentage GP and grafting efficiency GE were calculated to quantitatively evaluate the extent of acrylamide grafting onto the gum arabic backbone and the selectivity of the grafting process (Noordergraaf et al., 2018).

Determination of grafting parameters

GP represents the degree of backbone modification and was defined as the weight ratio of grafted polymer to the GA backbone, expressed as a percentage:

$$\mathrm{GP}\ (\%) = \frac{\mathrm{W_g}}{\mathrm{W_p}} \times 100 \qquad (1)$$

GE reflects the efficiency of the grafting reaction and was defined as the fraction of polymer formed as grafted chains relative to the total polymer produced:

$$\mathrm{GP}\ (\%) = \frac{\mathrm{W_g}}{\mathrm{W_{g+}W_h}} \times 100 \qquad (2)$$

where W_p is the initial dry weight of the gum arabic backbone, W_g is the weight of polymer chains covalently grafted onto the backbone, W_h is the weight of homopolymer formed during the reaction. The calculated GP and GE values are summarized in Table 1.

Table 1

Summarize the grafting percentage (GP) and grafting efficiency (GE) of GA-g-AM hydrogels synthesized using APS and AIBN initiators

GA-g-AM	APS (10%)	AIBN (10%)
GP (%)	91%	57%
GE (%)	78%	40%

Homopolymerization refers to the radical polymerization of acrylamide occurring independently in the reaction medium without attachment to the GA backbone, producing free p-AM chains. To ensure accurate determination of grafting parameters, the synthesized hydrogels were repeatedly washed with deionized water to remove soluble homopolymer and unreacted monomers. The samples were then dried in a laboratory oven at 40°C until constant weight before measurements were performed.

Investigation of Swelling Properties

The degree of swelling (D_s) of the synthesized GA-g-AM hydrogels was determined by immersing the dried samples in buffer solutions of different pH values, as well as in distilled water, at room temperature (Elbedwehy & Atta, 2020; Manaila & Craciun, 2024). The swelling behavior was monitored over various time intervals of 30 min; 1; 2; 3; 4; 5; 6 and 24 h to study the swelling kinetics and equilibrium behavior. At each predetermined time, the swollen hydrogels were removed, filtered through a 100-mesh sieve, and kept for 20 min to remove excess surface water. The samples were then weighed to obtain the swollen weight**,** while the dry weight before immersion W_0 used as a reference. The degree of swelling was calculated using the following equation:

$$\mathrm{D_s}(\%) = \frac{\mathrm{W_1 - W_0}}{\mathrm{W_0}} \times 100 \qquad (3)$$

where W_1 is the weight of the swollen hydrogel and W_0 is the initial dry weight of the sample.

Instrumentation

The structural and morphological characterization of the synthesized GA-g-AM copolymer was performed using Scanning Electron Microscopy (SEM). Dried hydrogel samples were fractured to expose their internal morphology and directly examined with a Carl Zeiss Sigma SEM, which provided detailed information on the surface topography of the copolymer network. To further investigate the structural features, X-Ray Diffraction (XRD) analysis was carried out using a Rigaku Miniflex 600 diffractometer. This technique allowed the identification of crystalline and amorphous domains within the hydrogel, providing insight into the influence of acrylamide grafting on the gum arabic backbone. FTIR spectra were recorded using a Nicolet iS10 spectrometer (Thermo Scientific) equipped with an ATR accessory (ZnSe crystal) over

the range 4000–500 cm^{-1} under standard acquisition conditions.

Results and discussion

Proposed Reaction Mechanism

The graft copolymerization of AM onto GA proceeds via a free-radical grafting-from mechanism, in which the polysaccharide backbone serves as the primary reactive substrate for macroradical formation followed by chain propagation (Bhattacharya & Misra, 2004; Cummings et al., 2019; Odian, 2004). AM functions as the vinyl monomer responsible for chain growth and network formation. The vinyl double bond (C=C) of AM readily participates in radical polymerization, while the amide group ($–CONH_2$) contributes to hydrogen bonding, hydrophilicity, and water retention within the hydrogel structure. These features enable efficient propagation of polymer chains and stabilization of the hydrated network (Odian, 2004). GA plays both structural and chemical roles in the reaction system. Structurally, GA acts as the macromolecular backbone of the hydrogel network. Chemically, its polysaccharide chains contain numerous hydroxyl (–OH) and carboxyl (–COOH) functional groups capable of undergoing hydrogen abstraction reactions, thereby enabling the formation of active radical sites directly on the backbone (Etxabide et al., 2018; Verbeken et al., 2003). Upon thermal activation, APS, which contains a persulfate peroxide bond (–O–O–), undergoes homolytic cleavage to generate highly reactive sulfate radical anions ($SO_4^{\bullet -}$). These radicals can abstract hydrogen atoms from hydroxyl groups on the GA backbone, producing macroradicals localized on the polysaccharide chains. The activated GA macroradicals subsequently react with the vinyl double bond of acrylamide, initiating the growth of poly(acrylamide) graft chains directly from the backbone. This pathway promotes a higher density of grafting sites and facilitates the formation of a more interconnected polymer network (Bhattacharya & Misra, 2004; Odian, 2004).

In contrast, AIBN, characterized by an azo functional group (–N=N–), decomposes thermally with the release of nitrogen gas to form carbon-centered radicals. These radicals primarily react with the vinyl double bond of acrylamide monomers, initiating polymerization mainly through monomer activation rather than direct backbone activation. As a result, chain growth may occur partially in solution prior to attachment to the polysaccharide matrix, potentially leading to a lower grafting site density and a comparatively less compact network structure (Odian, 2004).

The bifunctional crosslinker MBAA, containing two polymerizable vinyl groups, participates in the radical copolymerization during polymer chain propagation ,where its vinyl groups react with growing poly(acrylamide) radical chains. Through successive radical addition, MBAA forms covalent bridges between different polymer chains, generating crosslink junction points and converting the grafted polymer into a three-dimensional hydrogel network (Elbedwehy & Atta, 2020; Manaila & Craciun, 2024).

Accordingly, GA functions not only as a passive support but also as an active radical-reactive backbone governing graft initiation, while the initiator type controls the radical generation pathway and ultimately determines the network architecture and structural compactness of the resulting hydrogels (Lv et al., 2019; Sievers 2021).

Swelling Behavior

The swelling behavior of GA-g-AM hydrogels synthesized using APS and AIBN initiators was investigated in buffer solutions of different pH values as well as in distilled water at room temperature (25 ± 1^0C). The swelling degree was recorded at predetermined time intervals (30 min, 1, 2, 3, 4, 5, 6, and 24 h) in order to evaluate both swelling kinetics and equilibrium behavior.

Fig.1 shows the time-dependent swelling profiles of the hydrogels in the tested media. In all environments, a rapid initial swelling stage was observed during the first hours of immersion, followed by a gradual approach toward equilibrium. This behavior is typical of crosslinked hydrogel systems and reflects rapid solvent diffusion into the polymer network followed by slower relaxation of polymer chains (Hoffman, 2012; Li & Mooney, 2016; Peppas et al., 2000). Both APS- and AIBN-initiated hydrogels exhibited their maximum swelling degree at pH 2, reaching equilibrium swelling values of approximately 720 ± 5% and 1026 ± 5%, respectively. The higher swelling observed in the AIBN-initiated system suggests the formation of a comparatively looser and less densely crosslinked network, allowing increased water penetration and greater polymer chain mobility.

Figure 1
Time-dependent swelling behavior of GA-g-AM hydrogels synthesized using APS and AIBN initiators in buffer solutions of different pH values and in distilled water

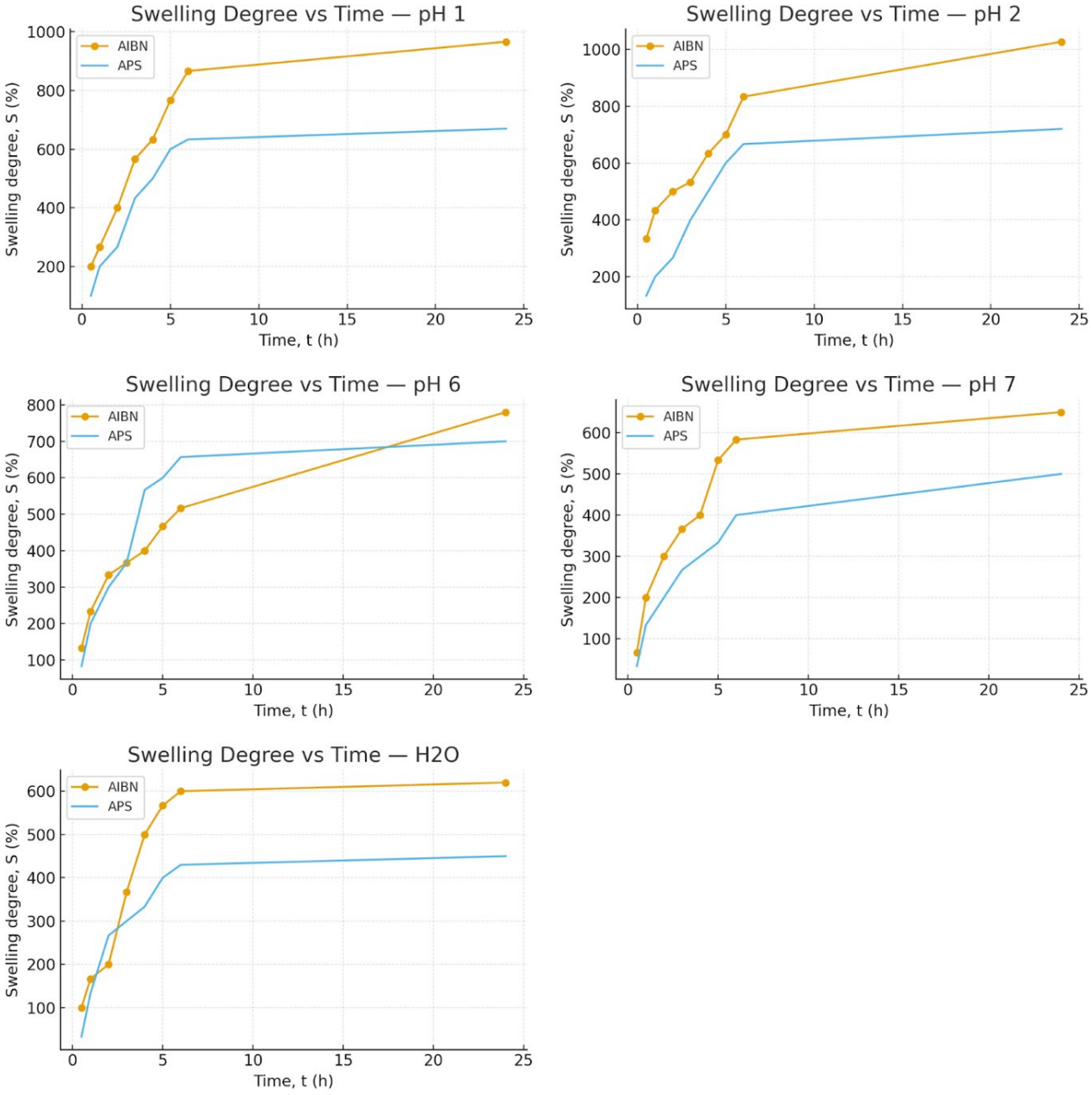

Conversely, the APS-initiated hydrogel displayed lower equilibrium swelling, which can be attributed to more efficient backbone activation and a higher density of grafting and crosslink junctions. The resulting compact network structure restricts free volume and limits solvent uptake (Sievers et al., 2021). All swelling measurements were performed in triplicate (n = 3), and the results are reported as mean ± standard deviation. When a crosslinked hydrogel is immersed in aqueous media of different pH values, it does not dissolve but absorbs water into its polymer network through diffusion. As water molecules penetrate the network, the hydrogel expands, leading to increased separation of polymer chains and enhanced segmental motion. The extent and rate of swelling are strongly influenced by the pH of the

surrounding medium, which affects the ionization state of functional groups within the network (Alonso et al., 2007; Navarro-Hermosillo et al., 2025).

The pH-dependent swelling behavior can also be interpreted considering the polyanionic nature of gum arabic. The presence of ionizable carboxyl groups generates fixed negative charges within the hydrogel network, producing an osmotic pressure difference between the polymer phase and the external solution (Donnan effect) (Li & Mooney, 2016; Peppas et al., 2000), which promotes water uptake and network expansion. Furthermore, the ionic strength of the surrounding medium influences the swelling equilibrium by screening electrostatic repulsion between charged groups, thereby modifying solvent diffusion and polymer relaxation processes.

In this study, the swelling kinetics of the synthesized GA-g-AM hydrogels were examined in buffer solutions of pH 1, 2, 6, and 7 at room temperature and at different time intervals. The experimental data were analyzed using the second-order kinetic model proposed by Schott (Noordergraaf et al., 2018), which can be expressed as:

$$\frac{t}{S_t} = A + B_t \quad (4)$$

where S_t is the swelling degree at time t , A is the intercept , and B_t is the slope of the linear plot. The parameter B_t represents the reciprocal of the equilibrium swelling degree

$$B = \frac{1}{S_E} \quad (5)$$

and the intercept A is related to the swelling rate constant

$$A = \frac{1}{k_s S_E^2} \quad (6)$$

The initial swelling rate can be expressed as:

$$k_{is} = k_s S_E \quad (7)$$

Thus, the Schott model can also be written in linearized form as:

$$\frac{t}{S_t} = \frac{1}{k_s S_E^2} + \frac{t}{S_E} \quad (8)$$

Linear plots of t/St versus t were constructed for each swelling medium and for both initiator systems (APS and AIBN). From the slope and intercept of the fitted lines, the equilibrium swelling degree S_E, swelling rate constant k_s, and initial swelling rate k_{is} were determined. The swelling kinetics were analyzed using the Scott second-order model. The calculated kinetic parameters are presented in Table 2, and the corresponding linear plots are shown in Fig. 2.

Table 2
Schott second-order swelling kinetic parameters for GA-g-AM hydrogels in different swelling media (mean ± SD, n = 3)

Medium	Initiator	S_E (g g^{-1})	k_s (g g^{-1} h^{-1})	k_{is} (g g^{-1} h^{-1})	R^2
pH1	AIBN	10.80	0.036	0.391	0.994
pH1	APS	7.51	0.056	0.419	0.986
pH 2	AIBN	12.00	0.031	0.367	0.991
pH 2	APS	8.12	0.046	0.374	0.987
pH 6	AIBN	8.90	0.030	0.263	0.989
pH 6	APS	8.03	0.038	0.303	0.995
pH 7	AIBN	7.46	0.044	0.326	0.981
pH 7	APS	6.10	0.036	0.216	0.951
H_2O	AIBN	7.05	0.054	0.377	0.971
H_2O	APS	5.21	0.066	0.344	0.938

Figure 2
Linear plots of the Schott second-order swelling kinetic model (t/S versus t) for GA-g-AM hydrogels synthesized using APS and AIBN initiators in different swelling media

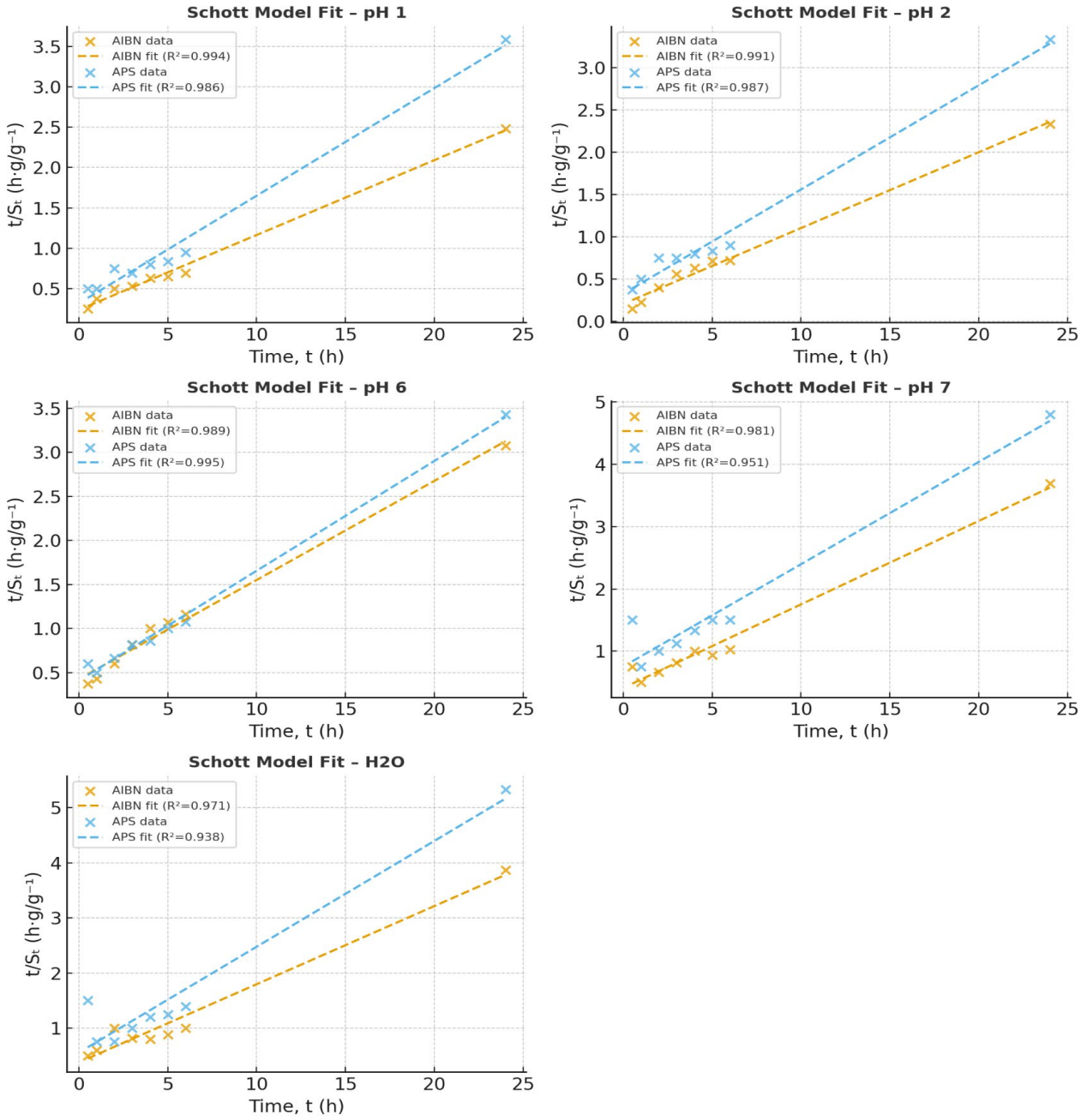

The high correlation coefficients (R^2 = 0.93–0.99) confirm that the Schott second-order kinetic model adequately describes the swelling behavior of the synthesized GA-g-AM hydrogels in all tested media. The results indicate that the swelling process is governed primarily by polymer network relaxation and solvent diffusion within the crosslinked structure (Peppas et al., 2000). Notably, the APS-initiated hydrogels exhibited more consistent kinetic parameters and a more controlled swelling profile, indicating the formation of a denser and structurally more stable polymer network (Lv et al., 2019; Sievers et al., 2021). In contrast, the AIBN-initiated hydrogels showed higher swelling capacity due to a comparatively looser network structure.

Characterization of the Prepared Hydrogels

Figure 3
FTIR spectra of (a) gum arabic, (b) acrylamide, (c) GA-g-AM (AIBN), and (d) GA-g-AM (APS)

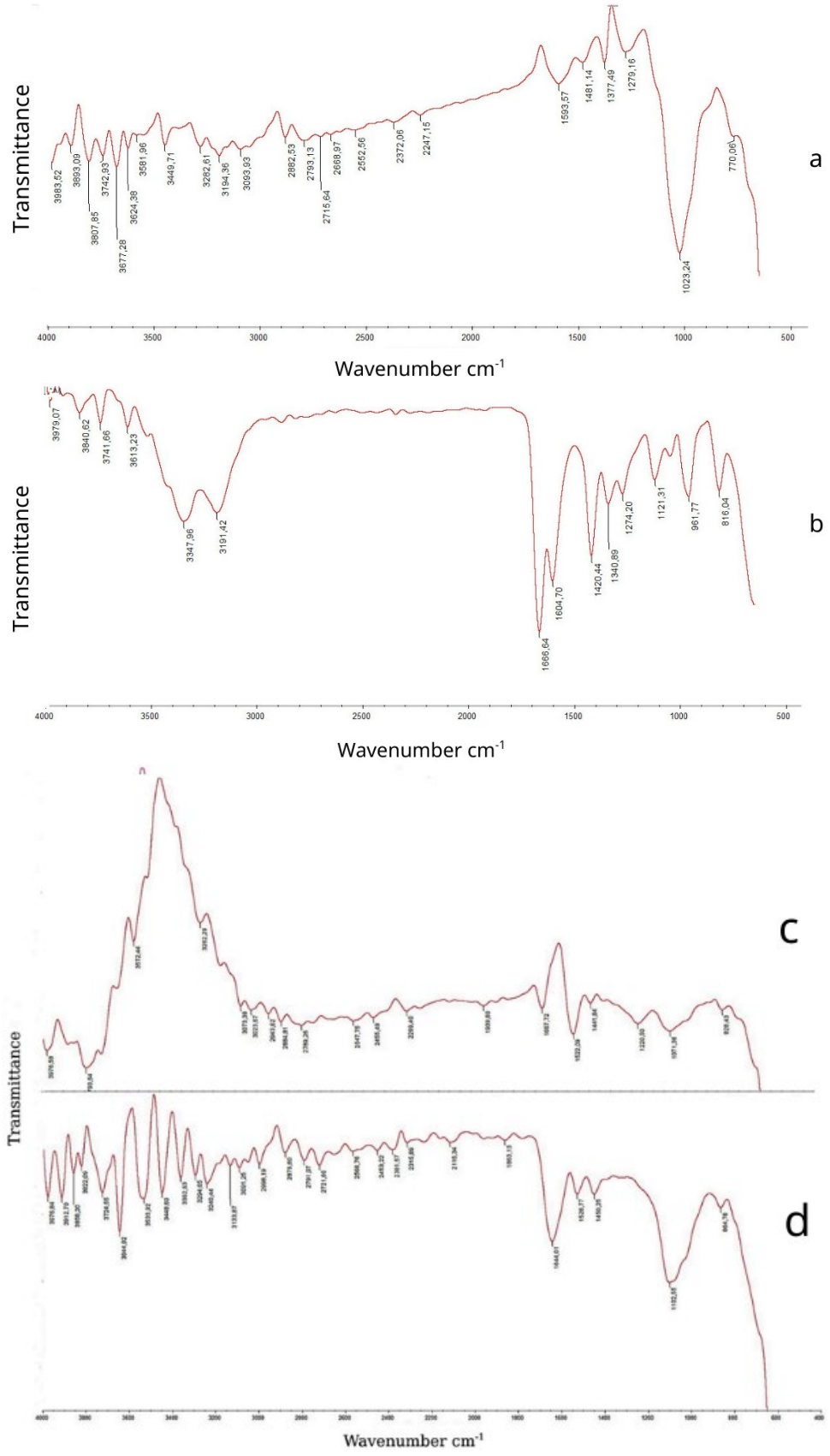

The FTIR spectra of native GA (Fig. 3a) and AM (Fig. 3b) were included for comparison to confirm the structural changes after graft copolymerization. The AIBN-initiated hydrogel (Fig. 3c) exhibited characteristic absorption peaks at 3572 and 3262 cm^{-1} corresponding to the stretching vibrations of –OH and –NH groups, confirming the presence of hydroxyl and amide functional groups. Peaks observed at 3073–2848 cm^{-1} were attributed to aliphatic C–H stretching vibrations. The distinct bands at 1667 and 1522 cm^{-1} were assigned to C=O (amide I) and N–H bending/C–N stretching (amide II), respectively, indicating the formation of amide linkages (Cao et al., 2011; Madduma-Bandarage & Madihally, 2021). Absorptions around 1220 and 1071 cm^{-1} were related to C–O–C and C–O stretching vibrations of the polysaccharide skeleton of GA, consistent with typical polysaccharide IR signatures (Etxabide et al., 2018; Verbeken et al., 2003). The spectrum exhibited relatively broader and less intense absorption bands, which may indicate differences in the local structural organization of the polymer matrix, potentially corresponding to a comparatively less compact network structure.

The APS-initiated hydrogel (Fig. 3d) displayed broad and intense absorption bands in the range of 3448–3724 cm^{-1}, attributed to overlapping –OH and –NH stretching vibrations, indicating the successful incorporation of hydrophilic functional groups during the grafting process. The prominent peaks at 1644 cm^{-1} (amide I, C=O stretching) and 1528 cm^{-1} (amide II, N–H bending/C–N stretching) confirmed the formation of amide linkages between GA and AM. The additional band at 1450 cm^{-1} corresponded to $–CH_2$ bending, while the sharp peak observed at 1102 cm^{-1} was assigned to C–O–C stretching of the polysaccharide backbone (Etxabide et al., 2018; Madduma-Bandarage & Madihally, 2021).

Comparative spectral analysis demonstrates that both initiators successfully induced graft copolymerization between GA and AM. However, the APS-initiated hydrogel exhibited sharper and more intense amide and hydroxyl bands compared to the AIBN-based sample, suggesting a comparatively higher grafting extent and a more densely crosslinked network. The enhanced intensity of these characteristic peaks is consistent with the formation of a more compact and structurally stable polymer matrix in the APS-initiated system.

Morphological analysis by SEM further supported these findings. The surface morphology of the synthesized hydrogels was examined by SEM, and the corresponding micrographs are shown in Fig. 4 (AIBN) and Fig. 5 (APS) (Kareem et al., 2021; Ostrowska-Czubenko et al., 2015).

The APS-initiated hydrogel exhibited a comparatively smoother, more compact, and homogeneous surface morphology, indicating a denser and more organized crosslinked network. The relatively uniform surface texture suggests efficient radical initiation and propagation during graft copolymerization, resulting in a tighter polymer matrix with reduced free volume. Such compact morphology is commonly associated with improved structural stability, lower porosity, and more restricted water mobility within the network (Jabrail & Mahmood, 2015; Ostrowska-Czubenko et al., 2015), which is consistent with the experimentally observed controlled swelling behavior. In contrast, the AIBN-initiated hydrogel exhibited a comparatively rougher and more irregular morphology, indicating a less uniform polymer network and a comparatively lower effective crosslink density. This more open structural configuration may facilitate increased water penetration and retention, consistent with the higher swelling capacity observed for the AIBN-based system (Bal et al., 2021; Franke & Gerlach, 2020; Kaberova et al., 2020).

It should be noted that SEM observations were performed on dried hydrogel samples; therefore, the observed morphology represents the dried state of the materials, and some structural shrinkage or pore deformation due to drying cannot be excluded of the surface features (Ibrahim et al., 2021; Sharma et al., 2022).

Figure 4
SEM analysis of GA-g-AM (AIBN)

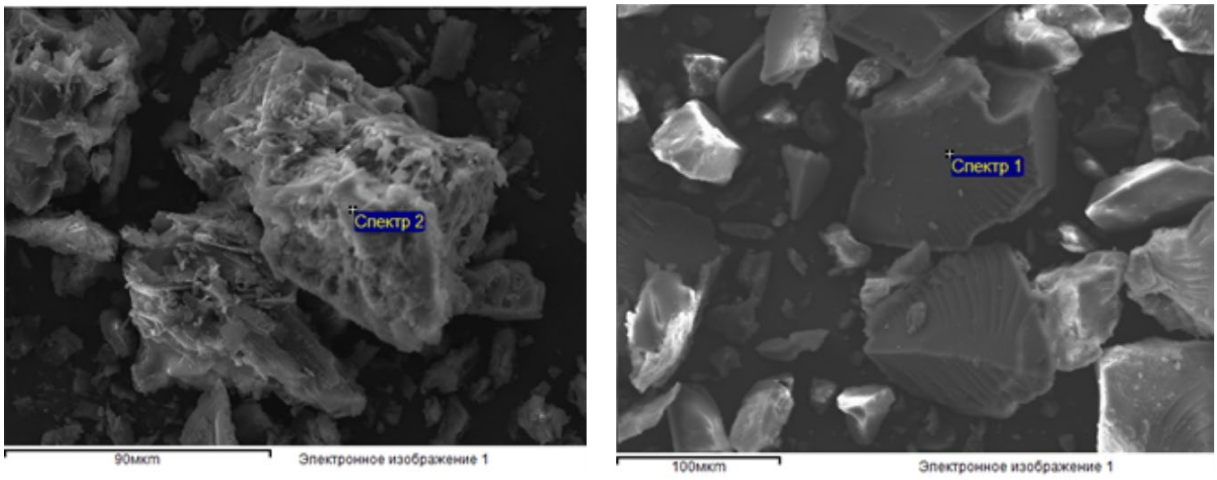

Figure 5
SEM analysis of GA-g-AM (APS)

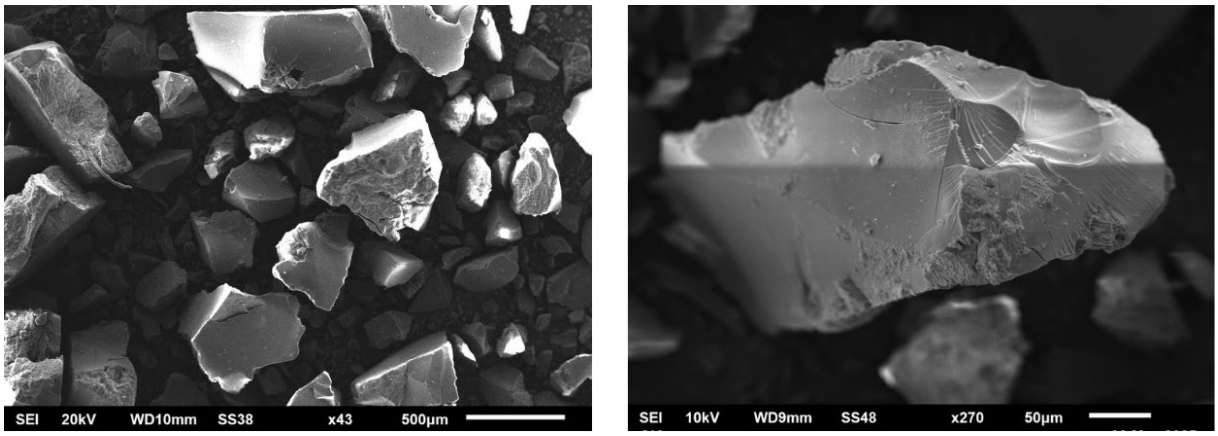

The XRD patterns of APS- and AIBN-initiated GA–g–AAm hydrogels showed broad halos around $2\theta \approx 20–25^0$, confirming their predominantly amorphous nature (Ibrahim et al., 2021; Kaberova et al., 2020). The slightly sharper and more intense peak in the APS-initiated sample indicates improved molecular ordering and denser crosslinking, while the broader halo in the AIBN-based hydrogel reflects a looser, less organized network (Kaberova et al., 2020; Ostrowska-Czubenko et al., 2015). These results confirm that APS produces a more compact and stable amorphous structure compared to AIBN. The XRD diffractograms of GA–g–AM hydrogels synthesized using APS (Fig. 6) and AIBN (Fig. 7) initiators are presented to illustrate the amorphous nature of the polymeric networks.

Figure 6
XRD spectrum of GA-g-AM (APS)

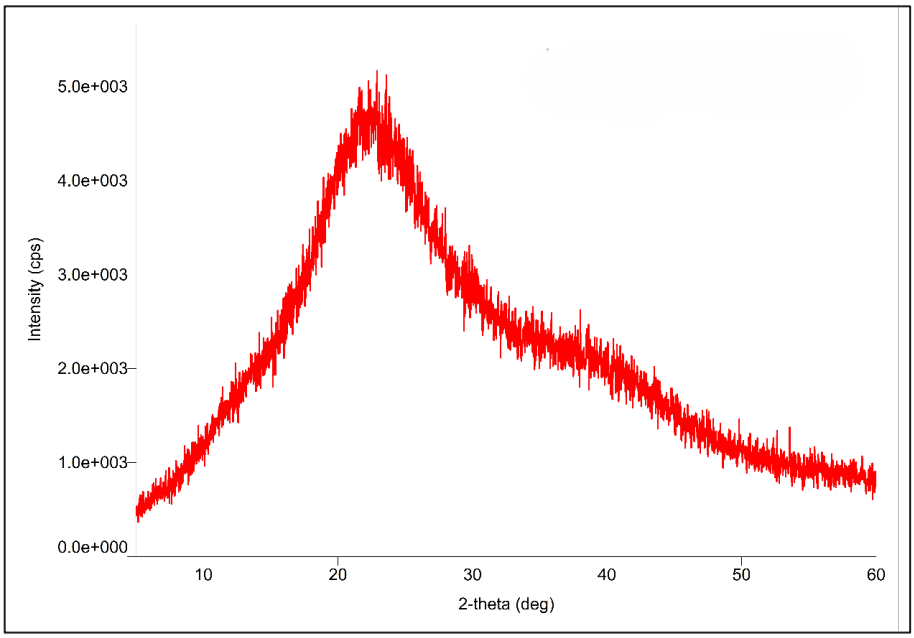

Figure 7
XRD spectrum of GA-g-AM (AIBN)

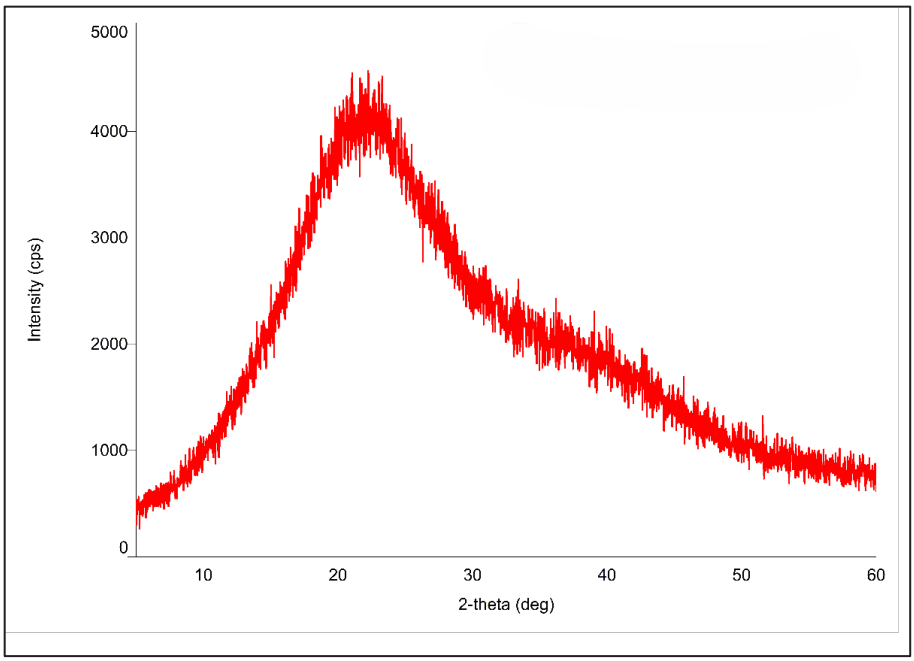

Conclusion

The FTIR spectra of the APS-initiated hydrogel exhibited stronger amide and hydroxyl absorption bands, confirming a higher degree of grafting. Morphological analysis through SEM further supported these findings, as the APS-grafted samples displayed a smoother, more uniform, and compact surface compared to the relatively rough structure observed in the AIBN-based hydrogel.

Overall, the results demonstrate that the initiator type plays a decisive role in governing the crosslinking process, network architecture, and swelling behaviour of GA-g-AM hydrogels. APS more effectively activates the gum arabic backbone and promotes the formation of a denser and more uniformly crosslinked three-dimensional polymer network. The higher crosslink density restricts polymer chain mobility and reduces free volume, resulting in improved structural stability and more controlled swelling behaviour, whereas AIBN leads to a comparatively looser and more absorbent polymer network.

Author contributions

E.F. Aliyeva: Conceptualization, Methodology, Investigation, Writing – Original Draft; N.T. Rahimli: Visualization; N.A. Zeynalov: Supervision.

Conflict of interest

The authors declare that there is no conflict of interest regarding the publication of this article.

References

1. Ali, B. H., Ziada, A., & Blunden, G. (2009). Biological effects of gum Arabic. *Food and Chemical Toxicology*, *47*(1), 1–8. https://doi.org/10.1016/j.fct.2008.07.001

2. Alonso, G., Rivera-Armenta, J. L., Mendoza, A. M., & Méndez-Hernández, M. L. (2007). Effect of temperature and pH on swelling behavior of hydroxyethyl cellulose–acrylamide hydrogel. *e-Polymers*, *7*(1), 1744. https://doi.org/10.1515/epoly.2007.7.1.1744

3. Amaya-Chantaca, N. J., Caldera-Villalobos, M., Claudio-Rizo, J. A., Pérez-Pérez, E., Hernández-Cocoletzi, H., & Álvarez-Ramírez, J. (2022). Semi-IPN hydrogels of collagen and gum Arabic with antibacterial capacity and controlled drug release. *Progress in Biomaterials*, *11*(2), 197–210. https://doi.org/10.1007/s40204-022-00210-w

4. Bal, T., Mesra, P., Singh, P., & Rajora, A. D. (2021). Polyacrylamide grafted gum acacia (GA-g-PAM) graft copolymer as efficient polymeric scaffold. *Indian Journal of Pharmaceutical Education and Research*, *55*(2s), s441–s447. https://doi.org/10.5530/ijper.55.2s.115

5. Bhattacharya, A., & Misra, B. N. (2004). Grafting: a versatile means to modify polymers. *Progress in Polymer Science*, *29*(8), 767–814. https://doi.org/10.1016/j.progpolymsci.2004.05.002

6. Cao, Y. F., Liu, Z. L., Li, Y., & Tan, F. Z. (2011). Graft copolymerization of starch and acrylamide initiated by AIBN in aqueous two-phase system. *Advanced Materials Research*, *239–242*, 1433–1436. https://doi.org/10.4028/www.scientific.net/AMR.239-242.1433

7. Çankaya, N. (2016). Synthesis of graft copolymers onto starch and its semiconducting properties. *Results in Physics*, *6*, 538–542. https://doi.org/10.1016/j.rinp.2016.08.010

8. Cummings, S., Zhang, Y., Smeets, N., Cunningham, M., & Dubé, M. A. (2019). On the use of starch in emulsion polymerizations. *Processes*, *7*(3), 140. https://doi.org/10.3390/pr7030140

9. Elbedwehy, A. M., & Atta, A. M. (2020). Novel superadsorbent highly porous hydrogel based on Arabic gum and acrylamide grafts for fast and efficient methylene blue removal. *Polymers*, *12*(2), 338. https://doi.org/10.3390/polym12020338

10. Etxabide, A., Téllez-Jurado, A., Martínez-Sanz, M., Villar, M., Eceiza, A., & Corcuera, M. A. (2018). Bioinspired alginate–gum Arabic hydrogel with controlled release capabilities. *ACS Applied Materials & Interfaces*, *10*(29), 24783–24793. https://doi.org/10.1021/acsami.7b04428

11. Franke, D., & Gerlach, G. (2020). Swelling studies of porous and nonporous semi-IPN hydrogels for sensor and actuator applications. *Micromachines*, *11*(4), 425. https://doi.org/10.3390/mi11040425

12. Gola, A., Bernardi, A., Pasut, G., & Musial, W. (2021). Influence of initiator concentration on properties of thermosensitive poly(acrylamide-co-AMPS) microparticles. *Polymers*, *13*(7), 996. https://doi.org/10.3390/polym13070996

13. Hoffman, A. S. (2012). Hydrogels for biomedical applications. *Advanced Drug Delivery Reviews*, *64*, 18–23. https://doi.org/10.1016/j.addr.2012.09.010

14. Ibrahim, S. M., Teo, Y. Y., & Misran, M. (2021). Synthesis, characterization and rheological study of Arabic gum-grafted-poly(methacrylic acid) hydrogels. *Polymer Bulletin*, *78*(11), 6087–6103. https://doi.org/10.1007/s00289-020-03267-4

15. Işıver, Y., & Saraydın, D. (2021). Smart hydrogels: preparation, characterization, and determination of transition points of crosslinked N-isopropyl acrylamide/acrylamide/carboxylic acids polymers. *Gels*, *7*(3), 113. https://doi.org/10.3390/gels7030113

16. Jabeen, S., Alam, S., Shah, L. A., & Zahoor, M. (2022). Removal of Safranin-T and Toluidine from water through gum arabic/acrylamide hydrogel. *Adsorption Science & Technology*, *2022*, 6100791. https://doi.org/10.1155/2022/6100791

17. Jabrail, F. H., & Mahmood, M. E. (2015). Hydrophilic monomers graft gum Arabic hydrogels prepared in different cross-linking nature and study of their effects on irrigation of agriculture soil. *Research Journal of Chemical Sciences*, *6*, 22–37.

18.Kaberova, Z., Karpushkin, E., Nevoralová, M., Vetrík, M., Šlouf, M., & Dušková-Smrčková, M. (2020). Microscopic structure of swollen hydrogels by scanning electron and light microscopies: artifacts and reality. *Polymers*, *12*(3), 578. https://doi.org/10.3390/polym12030578

19.Kareem, S. A., Dere, I., Gungula, D. T., Ajayi, A. H., & Olanrewaju, J. A. (2021). Synthesis and characterization of slow-release fertilizer hydrogel based on hydroxypropyl methyl cellulose. *Gels*, *7*(4), 262. https://doi.org/10.3390/gels7040262

20.Li, J., & Mooney, D. J. (2016). Designing hydrogels for controlled drug delivery. *Nature Reviews Materials*, *1*(12), 16071. https://doi.org/10.1038/natrevmats.2016.71

21.Lv, Q., Wu, M., & Shen, Y. (2019). Enhanced swelling ratio and water retention capacity for novel super-absorbent hydrogel. *Colloids and Surfaces A: Physicochemical and Engineering Aspects*, *583*, 123972. https://doi.org/10.1016/j.colsurfa.2019.123972

22.Madduma-Bandarage, U. S. K., & Madihally, S. V. (2021). Synthetic hydrogels: synthesis, novel trends, and applications. *Journal of Applied Polymer Science*, *138*(19), 50376. https://doi.org/10.1002/app.50376

23.Manaila, E., & Craciun, G. (2024). Poly(acrylic acid)–sodium alginate superabsorbent hydrogels synthesized by electron-beam irradiation—Part II: swelling kinetics and absorption behavior in various swelling media. *Gels*, *10*(9), 609. https://doi.org/10.3390/gels10090609

24.Naushad, M., Sharma, G., & Alothman, Z. (2019). Gum Arabic crosslinked poly(acrylamide) hydrogel nanocomposites. *Journal of Cleaner Production*, *241*, 118263. https://doi.org/10.1016/j.jclepro.2019.118263

25.Navarro-Hermosillo, A. B., Landázuri-Gómez, G., Soltero-Martínez, J. F. A., & Santos, C. (2025). Obtaining and characterizing poly(acrylic acid-co-acrylamide) hydrogels reinforced with cellulose nanocrystals. *Gels*, *11*(2), 144. https://doi.org/10.3390/gels11020144

26.Noordergraaf, I. W., Fourie, T. K., & Raffa, P. (2018). Free-radical graft polymerization onto starch as a tool to tune properties in relation to potential applications. *Processes*, *6*(4), 31. https://doi.org/10.3390/pr6040031

27.Odian, G. (2004). *Principles of polymerization* (4th ed.). Wiley.

28.Ostrowska-Czubenko, J., Gierszewska, M., & Pieróg, M. (2015). pH-responsive hydrogel membranes based on modified chitosan: water transport and kinetics of swelling. *Journal of Polymer Research*, *22*(7), 153. https://doi.org/10.1007/s10965-015-0786-3

29.Peppas, N. A., Bures, P., Leobandung, W., & Ichikawa, H. (2000). Hydrogels in pharmaceutical formulations. *European Journal of Pharmaceutics and Biopharmaceutics*, *50*(1), 27–46. https://doi.org/10.1016/S0939-6411(00)00090-4

30.Przesławski, G., Szcześniak, K. B., Gajewski, P., & Marcinkowska, A. (2022). Influence of initiator concentration on polymerization course of methacrylate bone cement. *Polymers*, *14*(22), 5005. https://doi.org/10.3390/polym14225005

31.Purohit, P., Bhatt, A., Mittal, R. K., Abdellattif, H. M., & Farghaly, T. A. (2023). Polymer grafting and its chemical reactions. *Frontiers in Bioengineering and Biotechnology*, *10*, 1044927. https://doi.org/10.3389/fbioe.2022.1044927

32.Saber-Samandari, S., Saber-Samandari, S., & Gazi, M. (2013). Cellulose-graft-polyacrylamide/hydroxyapatite composite hydrogel with possible application in removal of Cu(II) ions. *Reactive and Functional Polymers*, *73*(11), 1523–1530. https://doi.org/10.1016/j.reactfunctpolym.2013.07.007

33.Sharma, G., Kumar, A., Naushad, M., Dhiman, P., Thakur, B., García-Peñas, A., & Stadler, F. J. (2022). Gum acacia-crosslinked-poly(acrylamide) hydrogel supported C3N4/BiOI heterostructure for remediation of crystal violet dye. *Materials*, *15*(7), 2549. https://doi.org/10.3390/ma15072549

34.Sievers, J., Sperlich, K., Stahnke, T., Kreiner, C., Eickner, T., Martin, H., & Guthoff, R. F. (2021). Determination of hydrogel swelling factors by two established and a novel non-contact continuous method. *Journal of Applied Polymer Science*, *138*(18), 50326. https://doi.org/10.1002/app.50326

35.Vega-Hernández, M. Á., Cano-Díaz, G. S., Vivaldo-Lima, E., Rosas-Aburto, A., Hernández-Luna, M. G., Martinez, A., & Font, J. C. (2021). A review on the synthesis, characterization, and modeling of polymer grafting processes. *Processes*, *9*(2), 375. https://doi.org/10.3390/pr9020375

36.Verbeken, D., Dierckx, S., & Dewettinck, K. (2003). Exudate gums: occurrence, production and applications. *Food Hydrocolloids*, *17*(1), 9–21. https://doi.org/10.1016/S0268-005X(02)00077-1

37.Zaharia, M. M., Pispas, S., Bucatariu, F., & Mihai, M. (2024). Synthesis of thermoresponsive chitosan-graft-poly(N-isopropylacrylamide) hybrid copolymer and its complexation with DNA. *Polymers*, *16*(10), 1315. https://doi.org/10.3390/polym16101315

Information about the authors:

Elmira Aliyeva – PhD candidate, Laboratory of Nanostructured metal-polymer catalysts, Ministry of Science and Education Republic of Azerbaijan, Institute of Chemistry PLE (Baku, Azerbaijan, e-mail: elmira.aliyeva@kqki.science.az).

Nargiz Rahimli – PhD candidate, Laboratory of Nanostructured metal-polymer catalysts, Ministry of Science and Education Republic of Azerbaijan, Institute of Chemistry PLE (Baku, Azerbaijan, e-mail: nargiz.rahimli@kqki.science.az).

Nizami Zeynalov – Doctor of Chemical Sciences, Head of Laboratory of Nanostructured metal-polymer catalysts, Ministry of Science and Education Republic of Azerbaijan, Institute of Chemistry PLE (Baku, Azerbaijan, e-mail: nizami.zeynalov@kqki.science.az).

Received 28 March 2026;
received in revised form 26 May 2026;
accepted 9 June 2026